Supporting information for: Experimental study of CO_2 capture from air via steam-assisted temperature-vacuum swing adsorption with a compact kg-scale pilot unit

H.M. Schellevis and D.W.F. Brilman

1. Pilot unit design and operational parameters

The manuscript analyses the operation and performance of the kg-scale Direct Air Capture (DAC) pilot unit based on a certain set of experimental conditions and operational parameters. These parameters are referred to as the 'design' parameters. This can be considered as the base case scenario. Table 1 shows an overview of the design parameters for the reactor compartments and operational parameters of the 'design' case.

Table 1: Overview of design parameters for the kg-scale pilot DAC unit and operational parameters for the 'design' scenario. a) The heat transfer area is normalized by the volume of the reactor that is occupied by sorbent, hence without the volume occupied by the heating spirals and spacers.

Parameter	Value
Number of reactors (-)	4
Reactor diameter (cm)	40
Sorbent bed thickness (cm)	2.4
Specific heat transfer area[a)] (m^2 m_r^{-3})	150
Sorbent mass per reactor (kg_s)	1.2
Reactor mass (kg_r)	4.0
Mass of heat transfer medium (kg)	0.25
Heat capacity ratio (-)	1.59
Adsorption time (min)	152
Evacuation time (min)	1
Heating time (min)	10
Desorption time (min)	30
Cooling time (min)	9
Cycle time (min)	202
Cycles per day (day^{-1})	7.1
Adsorption temperature (°C)	21.6
Adsorption relative humidity (-)	0.19
Superficial gas velocity (m s^{-1})	0.11
Temperature of heating medium (°C)	110
Average pressure during desorption (mbar)	74
Purge gas flowrate (g min^{-1})	1.04

Figure 1 shows a schematic of the experimental setup. It consists of four parallel reactor beds of which three are always in the adsorption step and in the regeneration phase. The ambient temperature and relative humidity are measured near the air inlet and the CO_2 concentration of feed air is measured after the air blower. In addition, the CO_2 concentration is measured in the exit of each separate reactor and in the combined exhaust. The temperature inside the reactor is measured at six different locations with a different distance to a heat transfer surface to reflect the average temperature inside the reactor. The temperature in the cold and hot circuit is measured before and after the inline heater and air cooler. The desorption system consists of a co-current, relative to the air flow, steam purge at elevated temperature and reduced pressure. The temperature of steam is regulated during steam generation and the pressure is measured in the product gas stream before the vacuum pump. The flow to the storage vessel is measured via the pressure inside the vessel.

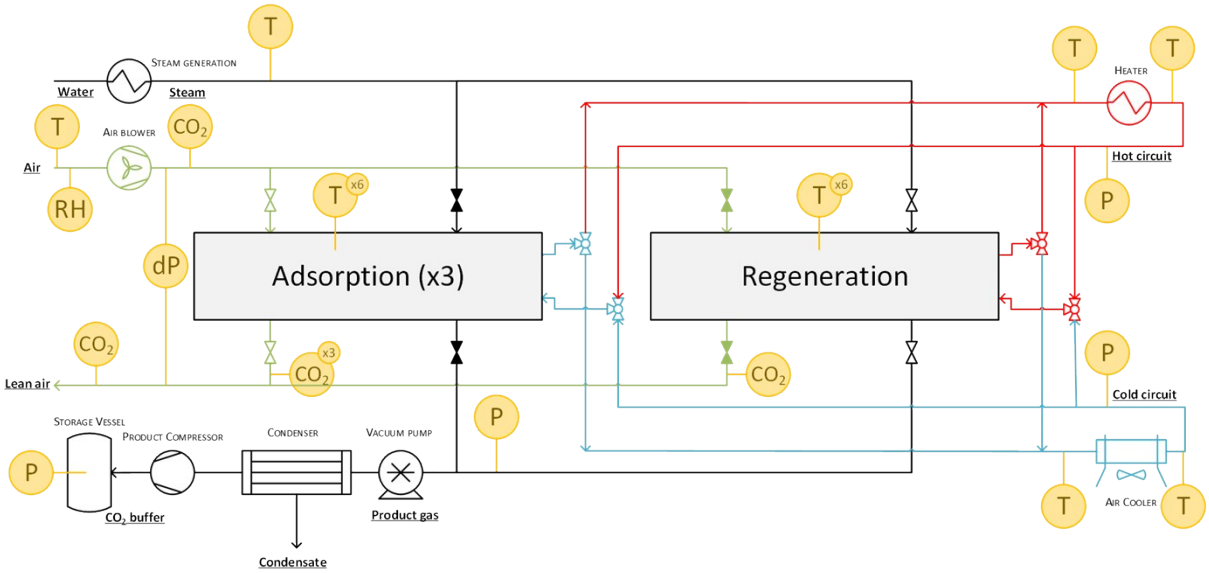

Figure 1: Schematic of the experimental setup including the locations of temperature, pressure, relative humidity and CO_2 concentration measurements.

2. Calculation of energy requirement and productivity

This chapter provides an overview of the calculations for the energy requirement of an S-TVSA cycle. Four parameters define a major part of the energy duty and these will be proposed first. Then, we introduce an equation to calculate each of the seven energy contributions based on these four parameters. This method can be applied to any (S-)TVSA cycle regardless of the gas-solid contacting method, sorbent of choice and reactor design. By comparing the four key parameters, it becomes convenient to evaluate different Direct Air Capture (DAC) processes.

The CO_2 working capacity ($^{\Delta q_{CO_2}}$), introduced in the main manuscript, is calculated via eq. (1) and is expressed in mol_{CO2}/kg_s. In this equation, $^{\Phi_{V,air}}$ is the volumetric air flowrate in m_g^3/min, $^{C_{CO_2}^{in}}$ is the inlet CO_2 concentration of air in mol_{CO2}/m_g^3, $^{C_{CO_2}^{out}}$ is the outlet CO_2 concentration of air in mol_{CO2}/m_g^3 and ^{m_s} is the sorbent mass of the bed in kg.

$$\Delta q_{CO_2} = \frac{\int \Phi_{V,air}\left(C_{CO_2}^{in} - C_{CO_2}^{out}\right)dt}{m_s} \quad (1)$$

The selectivity of CO_2 towards H_2O ($^{S_{CO_2}}$) is the first parameter, which is calculated with eq. (2). Here, we assume that H_2O is the only component besides CO_2 that adsorbs on the sorbent. When this is not the case, the selectivities of CO_2 towards the other components is required as well. $^{\Delta q_{H_2O}}$ is the working capacity of H_2O in mol_{H2O}/kg_s.

$$S_{CO_2} = \frac{\Delta q_{CO_2}}{\Delta q_{H_2O}} \quad (2)$$

The heat capacity ratio between the reactor and sorbent ($^{R_{sens,r}}$) is the second parameter (eq. (3)). In fact, heat capacity of the reactor refers to all non-active components of the system that are participating in the temperature swing. In this case, that are the stainless steel reactor segment and the heat transfer medium. In this equation, m is the mass in kg and C_p is the specific heat capacity in J/kgK of the reactor segment (r), heat transfer medium (m) and sorbent bed (s).

$$R_{sens,r} = \frac{m_r C_{p,r} + m_m C_{p,m}}{m_s C_{p,s}} \quad (3)$$

The amount of purge gas that is used to desorb a certain amount of CO_2 ($^{R_{purge}}$) is the third parameter (eq. (4)). This is a measure of how efficient the purge gas is used to desorb CO_2. It is expressed in mol_{purge}/mol_{CO2}, where ^{n_p} is the total amount of purge added to the reactor during the desorption in moles.

$$R_{purge} = \frac{n_p}{m_s \Delta q_{CO_2}} \quad (4)$$

The CO_2 capture efficiency ($^{\eta_{gas}}$) is the final parameter (eq. (5)). This is the fraction CO_2 of the ingoing air that is captured during adsorption. It is a measure for the total amount of air that is required to capture a certain amount of CO_2. Here, $^{t_{ads}}$ is the adsorption time in min and $^{C_{CO_2}}$ is the CO_2 concentration of the air in mol_{CO2}/m_g^3.

$$\eta_{gas} = \frac{m_s \Delta q_{CO_2}}{\Phi_{V,air} t_{ads} C_{CO_2}^{in}} \quad (5)$$

The energy requirements of the S-TVSA process will be expressed in J/kg_{CO2} and we divide this into seven categories:

- Adsorption enthalpy of CO_2
- Adsorption enthalpy of H_2O
- Sensible heat of the sorbent
- Sensible heat of the reactor
- Latent and sensible heat of the purge gas
- Feed compression
- Vacuum compression

The energy consumption for the endothermic desorption of CO_2 (E_{r,CO_2}) is determined by the molar reaction enthalpy ($\Delta_r H_{CO_2}$) and is given in eq. (6). This depends on the affinity of the CO_2 with the sorbent and is therefore a sorbent property.

$$E_{r,CO_2} = \frac{\Delta_r H_{CO_2}}{MW_{CO_2}} \tag{6}$$

The energy consumption for H_2O desorption (E_{r,H_2O}) is calculated from eq. (7). Here, $\Delta_r H_{H_2O}$ is the reaction enthalpy of H_2O in J/mol. The significance of H_2O co-adsorption is mostly determined by the selectivity, since a higher selectivity towards CO_2 will result in less energy consumption for H_2O desorption.

$$E_{r,H_2O} = \frac{\Delta_r H_{H_2O}}{S_{CO_2} MW_{CO_2}} \tag{7}$$

The sensible heat of the sorbent ($E_{sens,s}$) is calculated from eq. (8), where $C_{p,s}$ is the specific heat capacity of the sorbent in J/kgK. The temperature difference between adsorption and desorption (ΔT) depends on the ambient conditions and the choice for desorption temperature (or temperature of the heat transfer medium). The working capacity determines the number of cycles that is required to capture one kilogram of CO_2. A higher working capacity means that the sorbent is subject to less temperature swings and therefore require less energy for sensible heat.

$$E_{sens,s} = \frac{C_{p,s}\Delta T}{\Delta q_{CO_2} MW_{CO_2}} \tag{8}$$

The sensible heat of the reactor ($E_{sens,r}$) accounts for the temperature swing of all non-active material (eq. (9)). We relate this to the sensible heat of the sorbent via the heat capacity ratio (eq. (3)). This assumes the same temperature difference between adsorption and desorption as the sorbent.

$$E_{sens,r} = R_{sens,r} E_{sens,s} \tag{9}$$

The energy requirement of the purge gas (E_{purge}) consists of sensible heat and latent heat (eq. (10)). However, this only holds for a condensable purge gas, such as steam. When using for example nitrogen or air, it only requires sensible heat. Sensible heat is divided further into a liquid part and a gas part, where $C_{p,L}$ and $C_{p,G}$ are the specific heat capacities of the liquid and gas phase in J/kgK and ΔT_L and ΔT_G are the temperature increases of both these phases. This is determined by the desorption pressure, since the

boiling point reduces at reduced pressure. The evaporation enthalpy ($\Delta_{vap}H_{purge}$) in J/mol determines the amount of latent heat that is required. The purge gas ratio (R_{purge}) determines the total amount of energy that is required for purge gas generation.

$$E_{purge} = \frac{R_{purge}}{MW_{CO_2}}\left(MW_p C_{p,L}\Delta T_L + MW_p C_{p,G}\Delta T_G + \Delta_{vap}H_{purge}\right) \quad (10)$$

Feed compression (E_{feed}) is the amount of energy that is required for gas-solid contacting (eq. (11)). This assumes a constant gas velocity and constant CO_2 inlet concentration, although averaging out minor fluctuations will not result in a significantly different result. The pressure drop (ΔP) in Pa and the CO_2 capture efficiency determine amount of energy that is required. Furthermore, η_f is the efficiency of the air blower. The pressure drop can be considered as the fifth key parameter to compare direct air capture processes.

$$E_{feed} = \frac{\Delta P}{\eta_f C_{CO_2}\eta_{gas}MW_{CO_2}} \quad (11)$$

Vacuum compression (E_{vac}) is the final energy contributor of the direct air capture process. Eq. (12) assumes a constant temperature and pressure, which will not be the case. However, using the average values will give a good approximation of the energy duty to generate vacuum. It consists of three parts: CO_2 product gas, co-adsorbed H_2O and purge gas. The amount of energy required for the CO_2 product depends on the fraction of CO_2 in the product ($x_{CO_2}^{prod}$), for co-adsorbed H_2O it depends on the CO_2 selectivity and for the purge gas is depends on the purge gas ratio. Furthermore, η_{vac} is the efficiency of the vacuum pump, k is the C_p/C_v ratio, R is the gas constant in J/molK, $T_{des,av}$ is the time-average desorption temperature in K, P is the pressure of the product gas and $P_{des,av}$ is the average pressure during desorption.

$$E_{vac} = \frac{1}{MW_{CO_2}\eta_{vac}}\left(\frac{k}{k-1}\right)\left(\frac{1}{x_{CO_2}^{prod}} + \frac{1}{S_{CO_2}} + R_{purge}\right)RT_{des,av}\left(\left(\frac{P}{P_{des,av}}\right)^{\frac{k-1}{k}} - 1\right) \quad (12)$$

The productivity is expressed in two ways: by the total system productivity in kg_{CO2}/d to address the total capacity of the pilot unit and by normalizing by the sorbent mass with the productivity expressed in $kg_{CO2}/kg_s/d$. The former is calculated via eq. (13) as the sum of the productivities of each of the four reactors with t_{cycle} as total cycle time expressed in days. The latter is calculated by dividing the total productivity by the total amount of sorbent present in the system (eq. (14)).

$$Prod_{total} = \frac{\sum_{i=1}^{4}\Delta q_{CO_2,i}m_{s,i}}{t_{cycle}} \quad (13)$$

$$Prod_{total} = \frac{Prod_{total}}{\sum_{i=1}^{4} m_{s,i}} \tag{14}$$

3. Climate data – Enschede, The Netherlands

Ambient conditions are important for any Direct Air Capture (DAC) process as they determine the adsorption conditions. Temperature and relative humidity affect both reaction kinetics and equilibrium loading and therefore determine the adsorption rate. Figure 1 shows seasonal trends in temperature and relative humidity at the weather station at Twenthe Airport near Enschede[1]. A period of high relative humidity is nearly always present during a day, which will result in significant H_2O co-adsorption. Moreover, the variation within a single day can be substantial. This occurs predominantly during the summer as evident from the difference between daily maximum and daily minimum. Precipitation is common, but rather unpredictable. Obviously, during the precipitation the humidity level is high, leading to high H_2O co-adsorption values.

Figure 2 shows the occurrence of a combination of temperature and relative humidity throughout one year. These are obtained every hour and therefore give a good representation of the operational conditions during continuous operation of a DAC facility. The average temperature in this period was 10.2 °C and the average relative humidity was 81.8%. It shows that low temperature and low relative humidity do not coexist, same as a high temperature and high humidity. Most occurrences are at high relative humidity and in a temperature range of 5 to 20 °C. In contrast, the adsorption conditions during the experimental campaigns were not in this range. Conditions inside the laboratory ranged from 17 to 22 °C and 17 to 26% relative humidity. This especially influences the extent of H_2O co-adsorption, as this would be more extensive for outdoor experiments.

The mentioned yearly average temperature and relative humidity also do not give a good representation of year round operation, since a broad distribution occurs. The probability of a certain temperature or relative humidity to occur is shown in Figure 3. The temperature is mostly between 5 and 20 °C with outliers to −15 and 35 °C. The relative humidity shows a different profile, with a very small probability of a low relative humidity and almost 50% of the occurrences above 85% relative humidity.

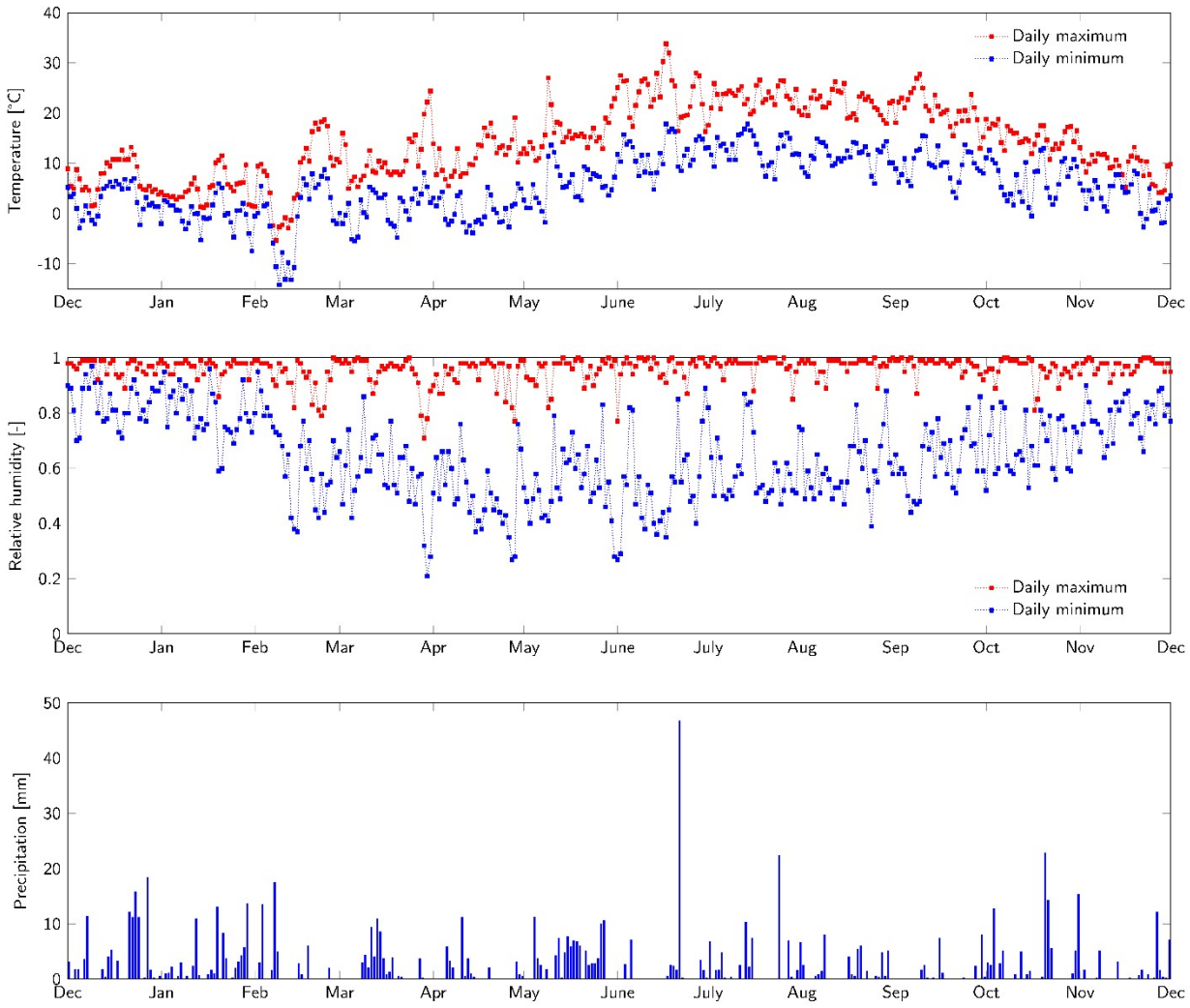

Figure 2: Daily weather data for Enschede, The Netherlands, from December 2020 until December 2021. The figures show the maximum and minimum temperature and relative humidity that was measured during a day. Furthermore, the total precipitation during a day is shown.[1]

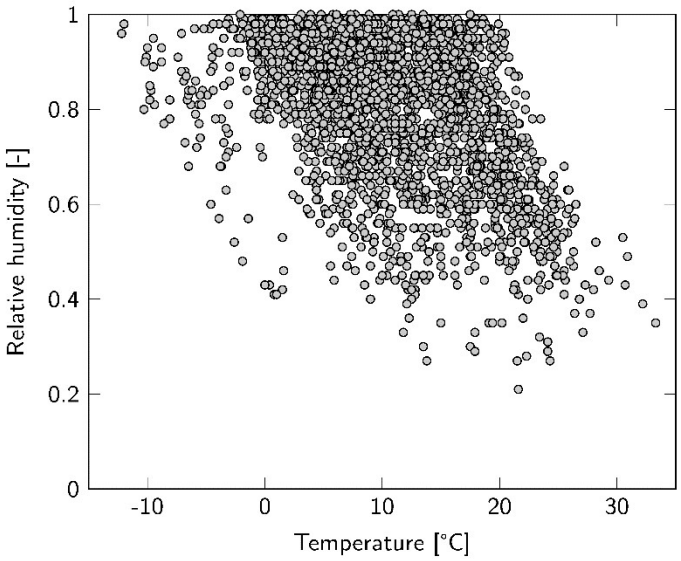

Figure 3: Occurrences of combinations of temperature and relative humidity. Based on hourly weather data from Enschede, The Netherlands from December 1st 2020 until December 1st 2021.

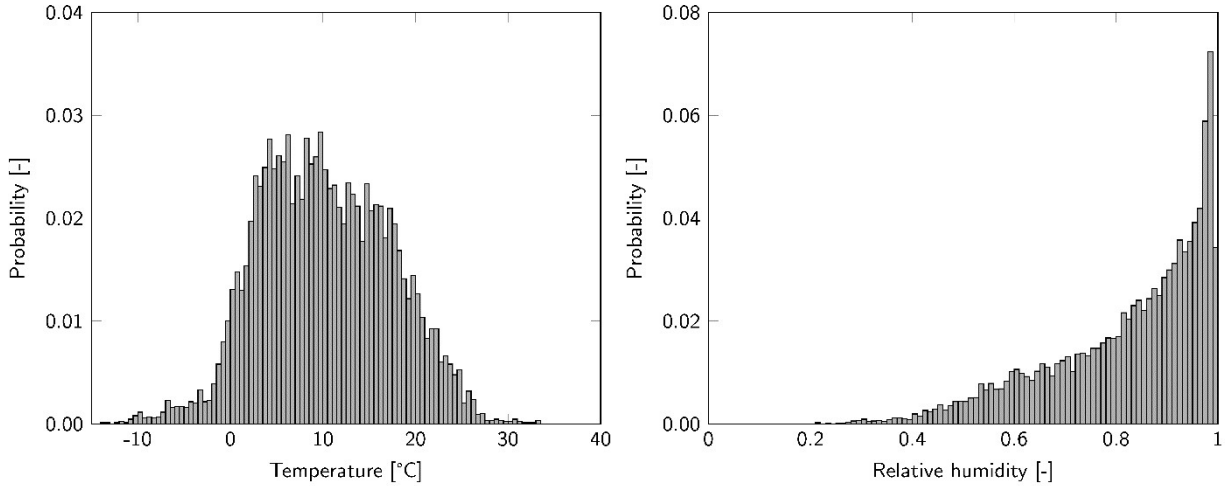

Figure 4: Probability of (A) a certain temperature (left) and (B) relative humidity (right) to occur.

4. Additional experimental results

This chapter contains additional experimental results of the experimental campaigns discussed in the manuscript. First, experimental results for the campaign with the 'design' parameter set are given to support the discussion and conclusions from sections 'Reproducibility' and 'Productivity'. Then, an overview of operational parameters and key performance indicators is provided for the effect of the purge gas flowrate. Finally, the experiments with a varying cycle length are compared in more detailed.

4.1. Experimental results using design parameter set

This section provides additional data to support the discussion regarding reproducibility and productivity. These are results from the experimental campaign with the 'design' parameter set, which can be found in ESI chapter 1. Figure 4 and Figure 5 show all breakthrough curves for each reactor. They all have a very

similar shape, but are not identical. This is due to a minor difference in gas flowrate between the reactors. This is taken into account in the calculation of the key performance indicators.

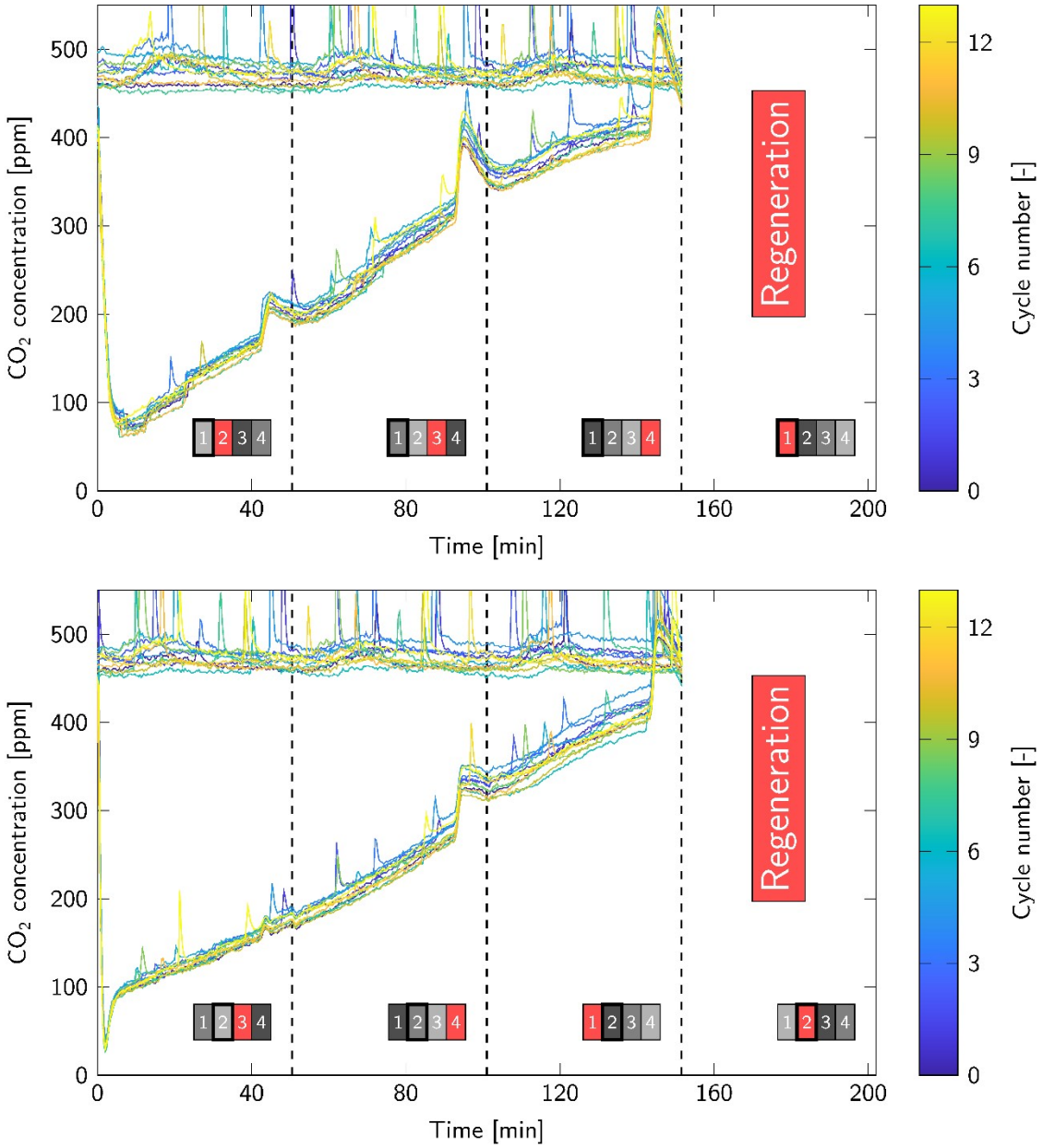

Figure 5: Breakthrough curves of reactors (A) 1 (top, identical to Figure 7 of the manuscript) and (B) 2 (bottom). The collection of graphs on the top are the ingoing concentration and the bottom graphs are the outgoing concentration. The dashed lines represent a switch in regeneration phase from one reactor to another; this is also indicated by the reactor scheme at the bottom. Here, a black/grey box represents the adsorption step and a red box represents a regeneration phase. The darker the box, the further along the adsorption step.

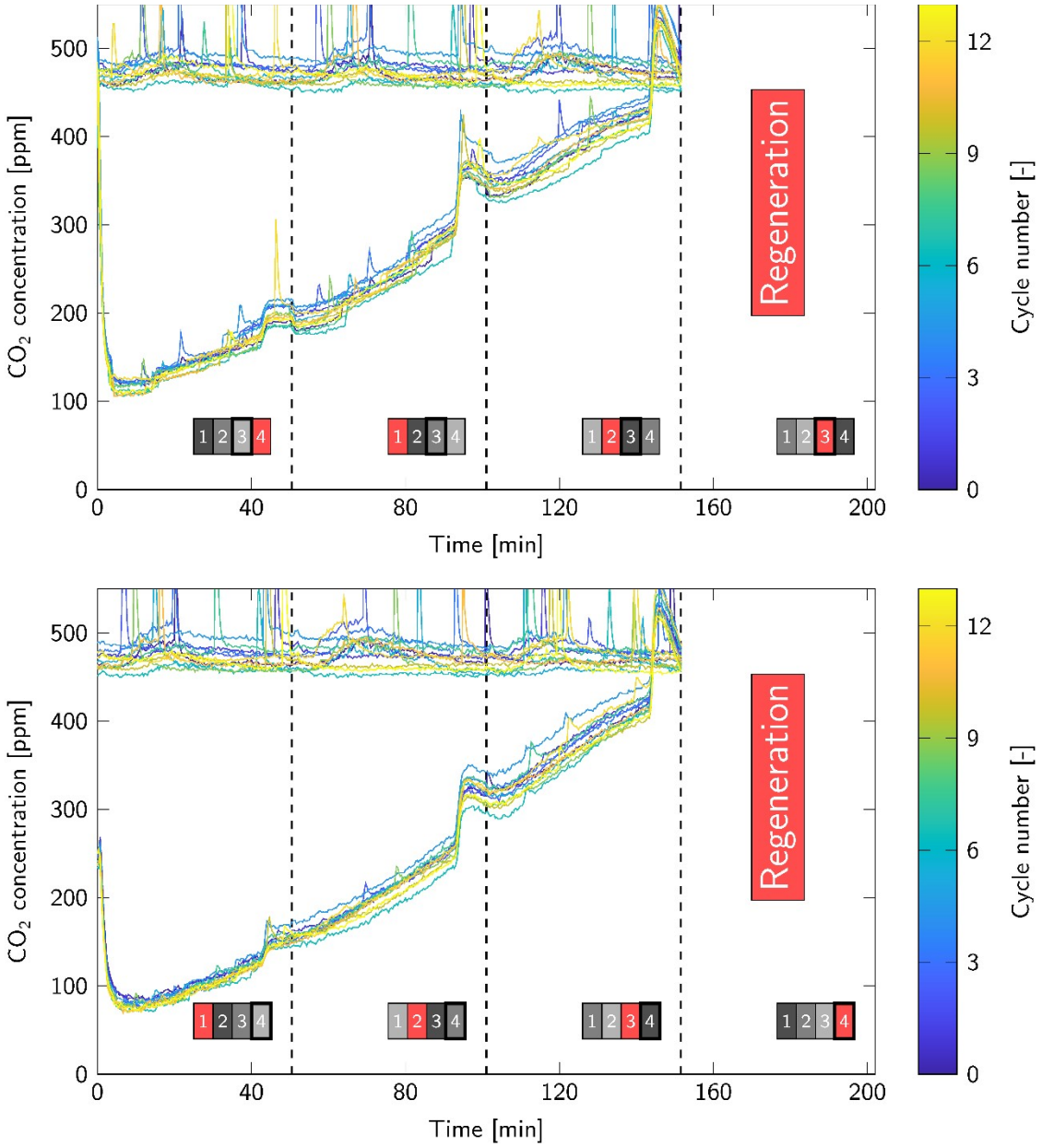

Figure 6: Breakthrough curves of reactors (A) 3 (top) and (B) 4 (bottom). The collection of graphs on the top are the ingoing concentration and the bottom graphs are the outgoing concentration. The dashed lines represent a switch in regeneration phase from one reactor to another; this is also indicated by the reactor scheme at the bottom. Here, a black/grey box represents the adsorption step and a red box represents a regeneration phase. The darker the box, the further along the adsorption step.

The breakthrough curves of all reactors show an increase in CO_2 outgoing concentration several minutes before a regeneration phase of another reactor ends. This is a result of a temperature increase in the reactors (Figure 6A). It occurs at the same moment the cooling step of another reactor starts. Then, the temperature of the cooling medium increases (Figure 6B), which also flows through the reactors that are in adsorption mode. The temperature of the cooling medium spikes at 40 °C which causes a 3 to 4 °C temperature increase in the reactors.

Figure 7A shows the temperature profiles of all reactors during regeneration. There are minor differences between the reactors that are most likely caused by the location of the thermocouples relative to the location of the heat transfer area. The temperature increase stops for a little while after approximately seven minutes of heating. This is due to a decrease in temperature of the heating medium (Figure 7B). Just after the heater, it drops to approximately 90 °C and will be a bit lower when entering the reactor due to heat losses to the environment. The graph shows only the average temperature; hence, the temperature at the interface of sorbent and heat transfer surface will be significantly higher.

All four reactors are identical in their design. However, manufacturing four identical reactors by hand is nearly impossible. Even though the performance of each reactor is very similar, the differences between reactors show in, for example, the vacuum pressure and pressure drop (Figure 8). The average pressure during the desorption step ranges from 64 mbar for reactor 2 to 88 mbar for reactor 4. The pressure drop differs depending on which reactors are simultaneously in adsorption step, although these changes are very small (within 10 Pa).

The standard deviation at a certain time of the cycles is indicated by a shaded area in all these figures. This again shows the reproducibility and stability of the Direct Air Capture (DAC) system. Especially for the temperature, where the shading is barely visible.

For completeness, Figure 10 shows the temperature profile of each cycle of reactor 1 during the complete cycle. Starting off with the adsorption step at 40°C that continues for ¾ of the cycle and finished with the regeneration phase that combines the evacuation, heating, desorption and cooling steps.

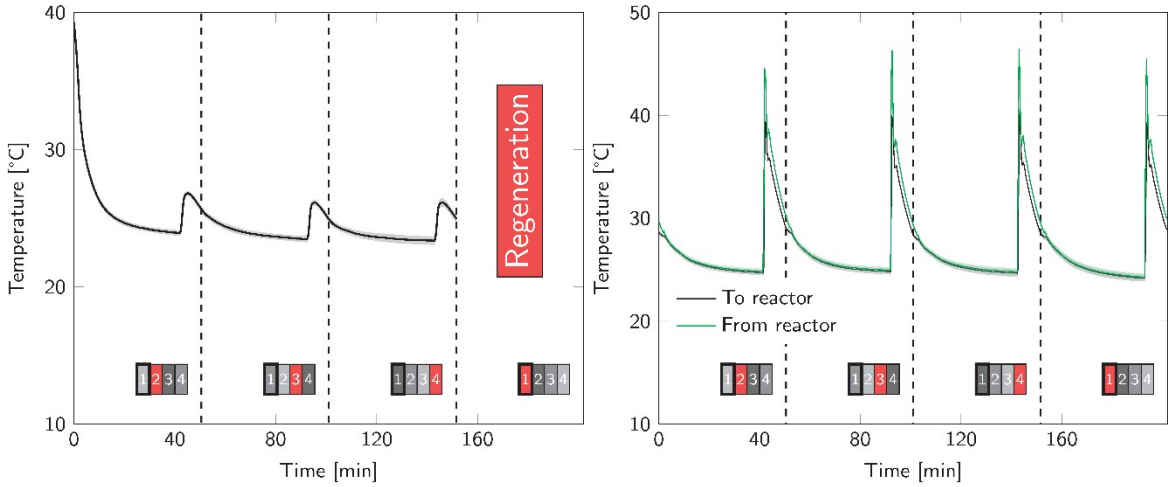

Figure 7: (A) Temperature of reactor 1 (left) and (B) temperature of the cooling medium (right) during the adsorption step. The dashed lines represent a change in reactor that is in regeneration mode. The shaded area is the standard deviation of all cycles.

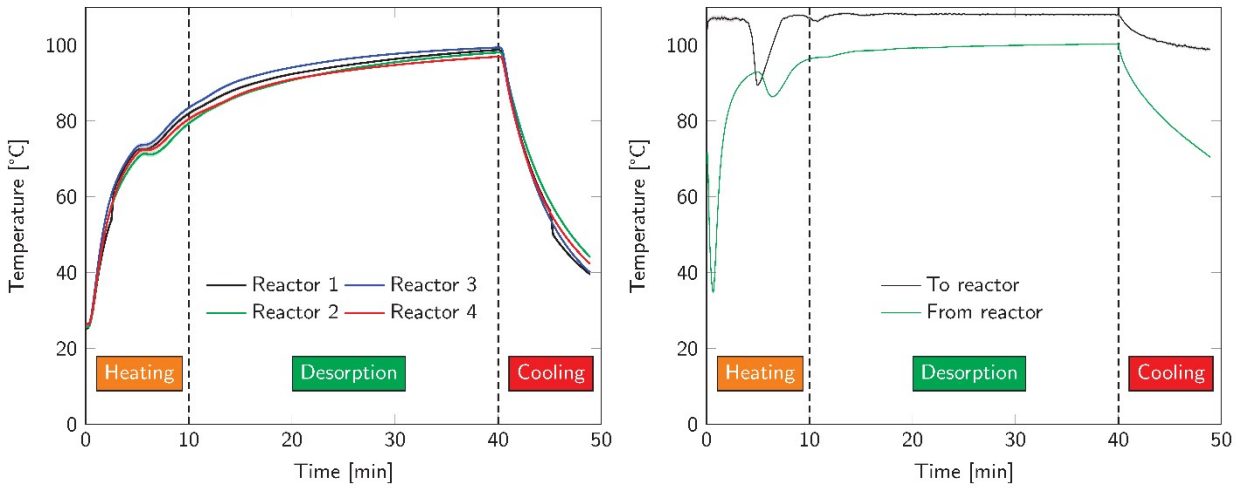

Figure 8: (A) Temperature of the reactors (left) and (B) heating medium during regeneration (right). The dashed lines identifies the heating, desorption and cooling step. The shaded area (although barely visible) is the standard deviation of all cycles.

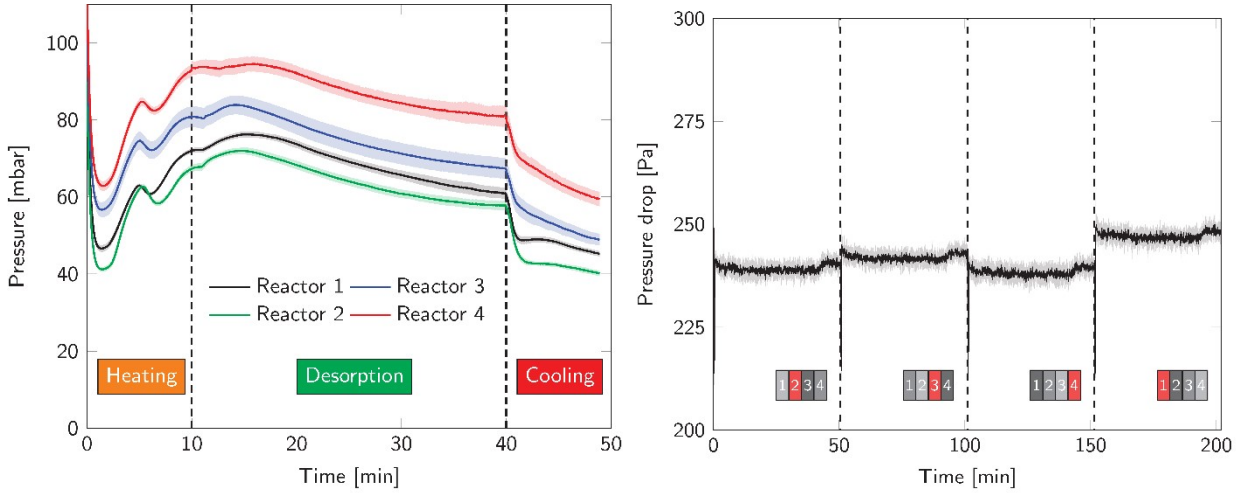

Figure 9: (A) Pressure during regeneration for all reactors (left) and (B) pressure drop during a complete cycle (right). The dashed lines in the left graph identifies the heating, desorption and cooling step. The dashed lines in the right graph represent a switch in regeneration phase from one reactor to another; this is also indicated by the reactor scheme at the bottom. The shaded area is the standard deviation of all cycles.

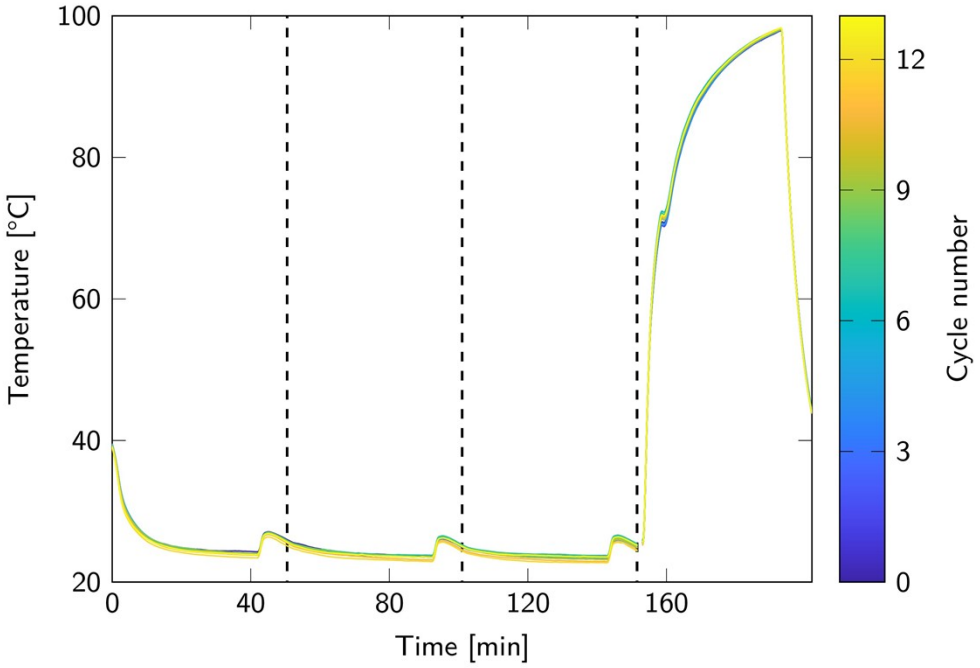

Figure 10: Temperature profile during complete S-TVSA cycle of reactor 1 for each cycle. The dashed lines represent a change in reactor that is in regeneration mode.

4.2. Effect of purge gas

The effect of purge gas flowrate on the performance of an S-TVSA process for DAC was evaluated. The experimental results using the 'design' parameters are compared to experimental results without the use of a purge gas. Table 2 gives an overview of the operational parameters and key performance indicators of both experiments.

Table 2: Overview of operational parameters and key performance indicators for the experiments with a steam purge and without a purge. Note that the 'Steam purge' parameters are identical to the 'design' parameters. a) This is the average pressure during desorption of reactors 1 to 3, since reactor 4 is not used in this comparison.

Parameter	**Steam purge**	**No Purge**
Adsorption time (min)	152	152
Evacuation time (min)	1	1
Heating time (min)	10	10
Desorption time (min)	30	30
Cooling time (min)	9	9
Cycle time (min)	202	202
Cycles per day (day^{-1})	7.1	7.1
Adsorption temperature (°C)	21.6	21.6
Adsorption relative humidity (-)	0.19	0.19
Superficial gas velocity ($m\ s^{-1}$)	0.11	0.11
Temperature of heating medium (°C)	110	110
Average pressure during desorption (mbar)	74	55[a)]
Purge gas flow rate ($g_{purge}\ min^{-1}$)	1.04	0
CO_2 working capacity ($mol_{CO2}\ kg_s^{-1}$)	0.92	0.82
H_2O working capacity ($mol_{H2O}\ kg_s^{-1}$)	1.04	1.06
CO_2/H_2O selectivity ($mol_{CO2}\ mol_{H2O}^{-1}$)	0.88	0.76
Productivity ($kg_{CO2}\ kg_s^{-1}\ day^{-1}$)	0.29	0.26
Pressure drop (Pa)	241	240
Purge gas ratio (mol_{purge}/mol_{CO2})	1.56	0
CO_2 capture efficiency (-)	0.42	0.39
Energy duty (MJ kg_{CO2}^{-1})	14.5	13.8
Reaction heat CO_2	*1.70*	*1.70*
Reaction heat H_2O	*1.12*	*1.28*
Sensible heat sorbent	*2.84*	*3.27*
Sensible heat reactor	*4.53*	*5.20*
Sensible and latent heat purge	*1.67*	*0.00*
Feed compression	*0.83*	*0.96*
Vacuum	*1.81*	*1.15*
Fraction thermal energy (-)	0.82	0.83
Fraction electrical energy (-)	0.18	0.17

4.3. Effect of cycle length

The cycle length was the final parameter that was varied and the main results are presented in the manuscript. This section first provides an overview of operational conditions and overall key performance indicators. Then, the effect is cycle length is assessed by comparing process parameters over time during a cycle.

Table 3 lists the operational conditions of each experimental campaign. The most notable difference, besides the adsorption and desorption time, is the relative humidity during the long cycles. This results in a 42% increase in H_2O working capacity.

Table 3: Summary of operational conditions and key performance indicators for the three different evaluated cycle lengths.

Parameter	**Short**	**Design**	**Long**
Adsorption time (min)	107	152	197
Evacuation time (min)	1	1	1
Heating time (min)	10	10	10
Desorption time (min)	15	30	45
Cooling time (min)	9	9	9
Cycle time (min)	142	202	262
Cycles per day (day^{-1})	10.1	7.1	5.5
Ambient temperature (°C)	18.3	21.6	18.6
Ambient relative humidity (-)	0.17	0.19	0.27
Superficial gas velocity ($m\ s^{-1}$)	0.11	0.11	0.11
Temperature of heating medium (°C)	110	110	110
Average pressure during desorption (mbar)	73	74	74
Purge gas flow rate ($g\ min^{-1}$)	1.04	1.04	1.04
CO_2 working capacity ($mol_{CO2}\ kg_s^{-1}$)	0.67	0.92	1.05
H_2O working capacity ($mol_{H2O}\ kg_s^{-1}$)	0.98	1.04	1.48
CO_2/H_2O selectivity ($mol_{CO2}\ mol_{H2O}^{-1}$)	0.69	0.88	0.71
Productivity ($kg_{CO2}\ kg_s^{-1}\ day^{-1}$)	0.30	0.29	0.25
Productivity ($kg_{CO2}\ day^{-1}$)	1.44	1.38	1.13
Pressure drop (Pa)	242	241	245
Purge gas ratio (mol_{purge}/mol_{CO2})	1.06	1.56	2.04
Capture efficiency (-)	0.44	0.42	0.36
Energy duty ($MJ\ kg_{CO2}^{-1}$)	16.4	14.5	14.9
Reaction heat CO_2	*1.70*	*1.70*	*1.70*
Reaction heat H_2O	*1.42*	*1.12*	*1.38*
Sensible heat sorbent	*3.74*	*2.84*	*2.55*
Sensible heat reactor	*5.95*	*4.53*	*4.06*
Sensible and latent heat purge	*1.14*	*1.67*	*2.19*
Feed compression	*0.80*	*0.83*	*0.97*
Vacuum	*1.68*	*1.81*	*2.06*
Fraction thermal energy (-)	0.85	0.82	0.80
Fraction electrical energy (-)	0.15	0.18	0.20

The analyses in the manuscript are mostly based on the overall key performance indicators. This section provides a more detailed analysis by comparing time-based profiles of process parameters. Figure 9A addresses the adsorption step where the breakthrough curves of each experiment are compared. The initial drop in CO_2 concentration relates to the initial CO_2 loading of the sorbent. This implies that the initial CO_2 loading is higher for the short cycle. Therefore, the short regeneration phase limits the productivity. The design and long cycle time follow a very similar curve. This indicates a very similar initial sorbent loading and the additional working capacity for the long cycle is obtained due the extended adsorption time. However, this is at a low adsorption rate, which causes the overall productivity to be lower. This is shown in Figure 9B, where the productivity decreases the furthest for the long cycle. Even though the CO_2 outgoing concentration of the short cycle is higher than the others, it still has the highest overall productivity since all reactors operate in a regime with a relatively high adsorption rate. The standard deviation of the results for the various cycles is visible through the shaded area. The breakthrough curves of the long cycle have a much larger standard deviation. This is due to a larger fluctuation of ambient CO_2 concentration. The productivity on the other hand does not show such a large standard deviation.

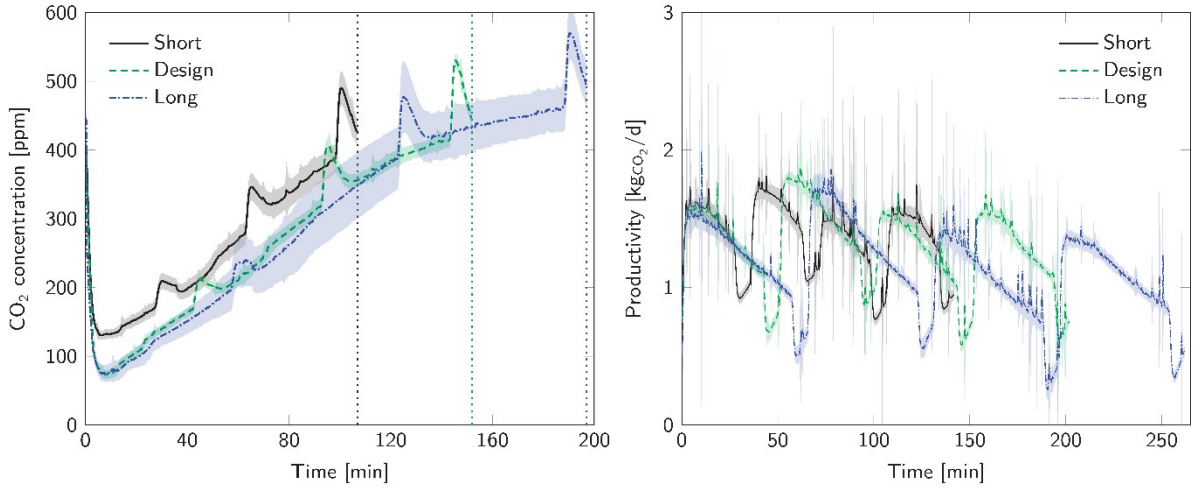

Figure 11: (A) Average breakthrough curves of reactor 1 for each cycle length (left) and (B) productivity during a complete cycle (right). Shaded areas represent the standard deviation of a cycle.

Figure 10 addresses the regeneration phase with a comparison of temperature and pressure profiles. The temperature profiles follow a very similar path. However, the temperature is a little higher with decreasing cycle length. This can be caused by the differences in CO_2 (and H_2O) working capacity. A higher working capacity means that more energy is spend to desorb the species and therefore less energy is left to heat up the sorbent.

The trend in desorption pressure is the same for all cycle lengths. Only at the end of the desorption step of the long cycle, some fluctuations in pressure occur. This is due water condensation inside the tubing between the reactors and the vacuum pump. More steam accumulates in the system for a longer desorption step and eventually it blocks the gas flow to the vacuum pump. This increases the pressure until a slug of product gas breaks through the blockage.

The pressure is higher for a longer cycle length after a certain amount of time. The higher working capacity, and thus amount of product gas, contributes to this phenomenon. In addition, water condensate

that is leftover from the previous cycle also has to be evaporated, which could result in a higher desorption pressure.

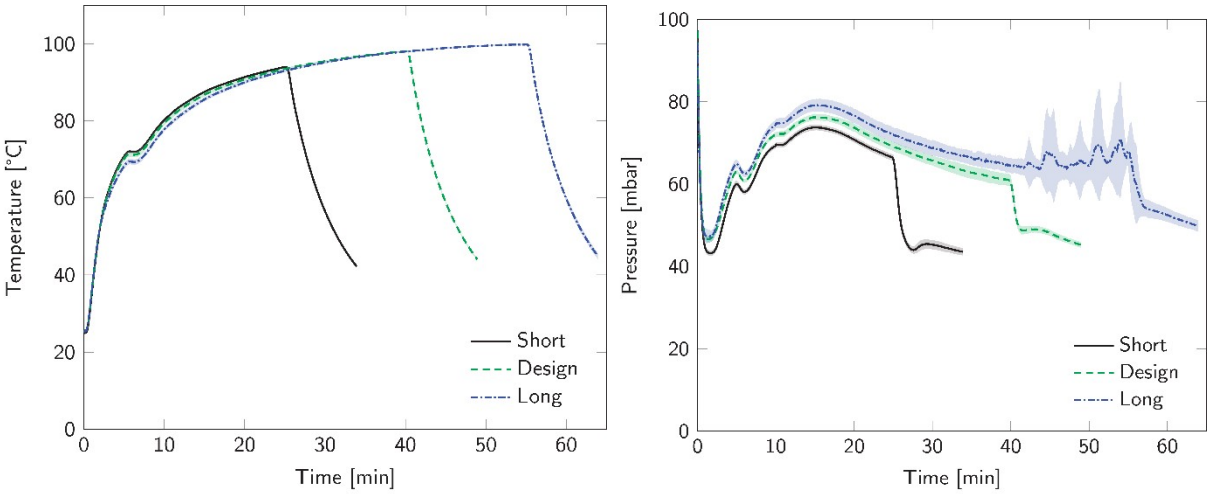

Figure 12: Comparison of the (A) temperature profile (left) and (B) pressure profile (right) of a single reactor during regeneration. Shaded areas represent the standard deviation of a cycle.

5. Nomenclature

Symbol	Description	Unit
C_{CO_2}	Gas phase CO2 concentration	$mol_{CO2}\ m_g^{-3}$
C_p	Specific heat capacity	$J\ kg^{-1}K^{-1}$
E_{feed}	Energy duty of feed compression	$MJ\ kg_{CO2}^{-1}$
E_{purge}	Energy duty of purge gas generation	$MJ\ kg_{CO2}^{-1}$
E_{r,CO_2}	Energy duty of CO_2 desorption	$MJ\ kg_{CO2}^{-1}$
E_{r,H_2O}	Energy duty of H_2O desorption	$MJ\ kg_{CO2}^{-1}$
$E_{sens,r}$	Energy duty of reactor sensible heat	$MJ\ kg_{CO2}^{-1}$
$E_{sens,s}$	Energy duty of sorbent sensible heat	$MJ\ kg_{CO2}^{-1}$
E_{vac}	Energy duty of vacuum generation	$MJ\ kg_{CO2}^{-1}$
$\Delta_r H$	Reaction enthalpy	$J\ mol^{-1}$
$\Delta_{vap} H$	Evaporation enthalpy	$J\ mol^{-1}$
k	Heat capacity ratio	-
MW	Molecular weight	$kg\ mol^{-1}$
m	Mass	kg
n_p	Total amount of purge gas added during a cycle	mol_{purge}
P	Pressure	Pa
$PROD_{norm}$	Productivity normalized by sorbent mass	$kg_{CO2}\ k_s^{-1}d^{-1}$
$PROD_{total}$	Total system productivity	$kg_{CO2}\ d^{-1}$
Δq_{CO_2}	CO_2 working capacity of an S-TVSA cycle	$mol_{CO2}\ kg_s^{-1}$
Δq_{H_2O}	H_2O working capacity of an S-TVSA cycle	$mol_{H2O}\ kg_s^{-1}$
R	Gas constant	$J\ mol^{-1}\ K^{-1}$
$R_{sens,r}$	Reactor heat capacity ratio	-

R_{purge}	Purge gas ratio	$mol_{purge}\ mol_{CO2}^{-1}$
S_{CO_2}	Selectivity of CO2 over H2O	$mol_{CO2}\ mol_{H2O}^{-1}$
T	Temperature	K
t	Time	s
t_{cycle}	Total S-TVSA cycle time in days	d
x^{prod}	Molar fraction of species in product gas	-
Greek symbols		
η_f	Air blower energy efficiency	-
η_{gas}	Gas efficiency – fraction of CO2 captured from air	-
η_{vac}	Vacuum pump energy efficiency	-
Φ_v	Volumetric flowrate	$m_g^3\ s^{-1}$
Subscripts and superscripts		
ads	Adsorption step	
air	Air feed	
av	Average	
CO_2	Carbon dioxide	
des	Desorption step	
G	Gas phase	
H_2O	Water	
in	Inlet stream of reactor	
L	Liquid phase	
m	Heat transfer medium	
out	Outlet stream of reactor	
r	Reactor	
s	Sorbent	

6. References

1 *Weerstations – Dagwaarnemingen*, https://daggegevens.knmi.nl/klimatologie/daggegevens, (accessed: June 2022)